

Sensorless Speed Control of PMSM Drives using dSPACE DS1103 Board

Jurifa Mat Lazi, Zulkifilie Ibrahim, SitiNoormiza Mat Isa, AnggunAnugerah,FizatulAiniPatakor, Raihana Mustafa

Faculty of Electrical Engineering
University Teknikal Malaysia Melaka
Co-email : jurifa@utem.edu.my

Abstract—This paper presents the hardware implementation of sensorless speed control of Permanent Magnet Synchronous Motor (PMSM) drives using dSPACE DS1103 board. dSPACE Real-Time Interface (RTI) is the link between software and hardware development. It automatically implements the MATLAB/Simulink model on the dSPACE Expansion Box. The simplified mathematical model of the Permanent Magnet Synchronous Motor (PMSM) is also developed in this paper. Speed and torque controls of permanent magnet synchronous motors are usually attained by the application of position and speed sensors. Yet, speed and position sensors require the additional mounting space, reduce the reliability in harsh environments and increase the cost of the motor. Therefore, many studies have been performed for the elimination of speed and position sensors. Therefore, a V-I model based on adaptive control is proposed. A speed and position estimator is formed using parameter uncertainty cancellation to estimate the speed without using any sensor. Firstly, the speed estimation errors of a voltage and current model-based adaptive speed due to the parameter variation are analyzed. Consequently, an adaptation mechanism model is developed to cancel the effects of parameter variations on the estimated speed performance. Finally, the speed control with quantitative control performance considering the effect due to the feedback of estimated speed is presented. The experimental results prove that the speed and position estimator is capable to control the PMSM drives for variation of speed command and can be control during zero speed operation.

Keywords—dSPACE DS1103, vector control, PMSM, sensorless

I. INTRODUCTION

In Permanent Magnet Synchronous Motor, it is necessary to know the information of speed and rotor position for the implementation of vector control or field-oriented control with fast dynamic response, accurate speed regulation and high efficiency. Various techniques in sensorless strategy are discussed by different researchers. Most of the techniques are based on the voltage equations of the PMSM and the information of the terminal quantities, such as line voltage and phase current. By using this information, the rotor angle and speed are estimated directly or indirectly. Basically, estimation of the sensorless techniques can be based on different

categories; Back Electromagnetic Force, Excitation Monitoring, Motor Modification, Magnetic Saliency, Observer and Signal injection.

A. Sensorless

Back electromagnetic force (EMF) information can be used in brushless DC drive systems, where at any one time only two of the three phases are conducting. The direct back EMF detection method uses measurements of the instantaneous voltage across the third, non-conducting phase. If the drive is designed such that the non-conducting phase current reduces rapidly, then the back EMF can be measured directly across the non-conducting phase. The zero crossing of the phase voltage can then be used to generate commutation data. Detail explanation about principle of this approach is described in [1] and [2]. Back EMF estimation for the rotor speed offers satisfactory performance at higher speed. This method requires simple algorithm and uses less computational time.

Excitation monitoring schemes involve monitoring the conduction paths of the current through the inverter. One method is to monitor the conduction state of the inverter's anti-parallel free-wheeling diodes [3]. In a brushless DC motor, at any instant, only two phases are conducting with commutation for each 60° (electrical degrees). The system operates by chopping one switching signal and leaving the other devices on continuously. The back EMF voltage of the non-switching phase is then measured and when this voltage crosses zero, a commutation position is detected. As mentioned previously, by using back EMF, this approach suffers at low speed operation. This method exploits the saliency of the motor to extract the value of rotor position. Thus, makes this method not suitable for surface mounted PMSM. It is only suitable for salient pole motor only. This method also requires of extra hardware implementation due to the purpose of signal injection. However the main attraction of this method is it is very reliable at zero speed. This method can be tested by either using voltage space phasor or using current space phasor [4].

Observer-based systems allow the controller to access states which are not directly measurable. For example, flux linkage is not a directly measurable quantity. So, to obtain the flux linkage, the motor's phase voltages and currents are measured.

These, can be used together with the phase resistance, to obtain an estimation of flux-linkage via integration. [5] applied this technique to a surface mounted PMSM, where EMF is estimated from the measurement of terminal voltages and stator currents and is then processed to produce the stator flux linkage space vector. The angle of this vector is used to produce the stator current command signals. The system also uses the rate of change of the flux linkage angle to obtain a speed signal. Another class of observers uses the Extended Kalman Filter (EKF) to estimate both position and speed in real time [6]. The main drawback of this method is the requirement of extra hardware and need of huge memory, thus it need appropriate processor because of it deals with high sampling frequencies.

Another method [7-9] is using model references adaptive control (MRAC). MRAC computes a desired state (called as the functional candidate) using two different models (i.e. reference and adjustable models). The error between the two models is used to estimate an unknown parameter (here speed is the unknown parameter). Hence, there is many more speed estimation techniques have been reported in literature such as Back-EMF based method, Artificial Intelligent (AI), State observer based method and etc.

This current study introduces a sensorless technique using back EMF method based on differential of d-q currents and voltages to estimate the speed of the motor. The basic diagram for overall block diagram is depicted in Fig. 1. This figure shows the overall block diagram of the proposed method which consist PMSM, Voltage Source Inverter (VSI), speed controller, current controller and the speed and position estimator.

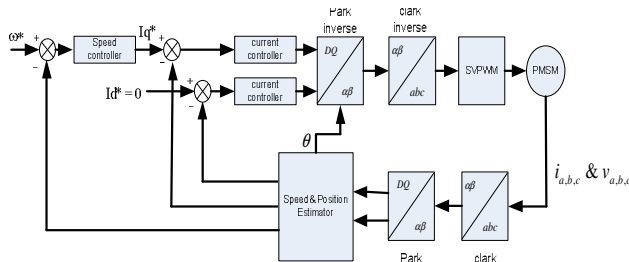


Fig. 1. Block diagram of Sensorless Speed Control of PMSM drives.

The above picture shows the basic configuration of Space Vector Pulse Width Modulation (SVPWM) for PMSM. Firstly, the speed controller estimates the torque through reference current, i_q^* , then, two current controllers convert the i_q^* and i_d^* signals to voltages (V_q^* , V_d^*). These voltages are then, transform to α - β model by using inverse Park's transformation. Then, using inverse Clark's equation, V_α^* and V_β^* , are converted to three phase voltages, V_a, V_b, V_c . These signals are used to generate SVPWM pulses before they can be used to drive a PMSM. The output three-phase voltages and currents are measured. These currents and voltages are being used in the speed estimator. The estimator will produce the estimated

value of motor's speed. The estimated rotor position is calculated by integrating the value of the motor speed. As a feedback, three-phase current outputs need to be transformed back to DQ model by using Clark and Park's equations. Finally, the actual i_d and i_q will be compared with the references current before resuming by the current controller.

B. dSPACE DS1103 Board

The combination of digital signal processors (DSPs) with the sophisticated power electronics controller have significantly contributed to the development of high performance permanent magnet synchronous motor (PMSM) drives [10-12]. The DSPs are commonly used to implement real-time and to control power electronic devices. The vector controlled PMSM drives is meeting the necessity of High Performance Drives (HPD) with the criteria of faster and accurate speed response, quick recovery of speed from any disturbances and insensitivity of parameter variations [13, 14].

dSPACE Real-Time Interference (RTI) is the link between the software development and dSPACE hard-ware. It automatically implements the MATLAB/Simulink on modular hardware installed in the dSPACE Expansion Box. If function modifications are necessary during the test, it can simply correct the function in Simulink and flash it to hardware again. The dSPACE prototyping system substitutes any controller and its connections to the vehicle or the controlled system during the development process.

II. MODELING OF PMSM DRIVES

The mathematical model of PMSM is derived from the synchronous motor under assumptions of saturation is neglected although it can be taken into account by parameter changes, the induced EMF is sinusoidal, eddy currents and hysteresis losses are negligible, no field current dynamics and no cage on the rotor [15].

The mathematical model for a PMSM in d-q reference frame can be determined by following equations [9],[16].

$$v_{dA} = r_{sA} i_{dA} + \frac{d}{dt} \psi_{dA} - \omega_e \psi_{qA} \quad (1)$$

$$v_{qA} = r_{sA} i_{qA} + p \psi_{qA} + \omega_e \psi_{dA} \quad (2)$$

Where:

v_d, v_q : d-q axis voltage

i_d, i_q : d-q axis currents

ω_e : electrical speed of motor

r_s : stator resistance

Ψ_d, Ψ_q : d - q axis flux linkages

The flux linkages Ψ_d and Ψ_q can be expressed in term of stator currents and constant flux linkage Ψ_m due to rotor permanent magnet as:

$$\Psi_{dA} = L_{dA} i_{dA} + \Psi_{mA} \quad (3)$$

$$\Psi_{qA} = L_{qA} i_{qA} \quad (4)$$

Where:

L_d, L_q : d - q axis inductances

By substituting equation (3) and (4) into equation (1) and (2), the new equations for stator voltages are formulated:

$$v_{dA} = r_{sA} i_{dA} + L_{dA} \frac{d}{dt} i_{dA} - \omega_e L_{qA} i_{qA} \quad (5)$$

$$v_{qA} = r_{sA} i_{qA} + L_{qA} \frac{d}{dt} i_{qA} + \omega_e L_{dA} i_{dA} + \omega_e \Psi_{mA} \quad (6)$$

The electromagnetic torque is

$$T_{emA} - T_{LA} = J \frac{d\omega_{rA}}{dt} \quad (7)$$

$$\text{with } T_{emA} = \frac{3}{2} p \times \text{real}\{i_A \Psi_{rA}\} \quad (8)$$

And the instantaneous angular position is;

$$\omega_{rA} = \frac{d\theta_A}{dt} \quad (9)$$

Stator current space vector with respect to the stationary phase magnetic axes is defined as:

$$i_s = i_s e^{j\phi} \quad (10)$$

Since the flux produced by permanent magnets has been assumed to be constant, the electromagnetic torque can be varied by changing the magnitude and the phase of the stator current. Thus, a constant torque is obtained if the quadrature axis component of the stator current space vector is kept constant and the max torque per Ampere of stator current is obtained if the torque angle is 90° . This corresponds to the application of imaginary axis only for the above stator current equation.

III. DESIGN OF SPEED AND POSITION ESTIMATOR

Fig. 2 represents the configuration of speed and position estimation scheme[9]. It consists of three-phase to two-phase conversion, adjustable model and adaptation mechanism. The

goals in the design are reducing the noise impact to control and influence the system transient response as small as possible.

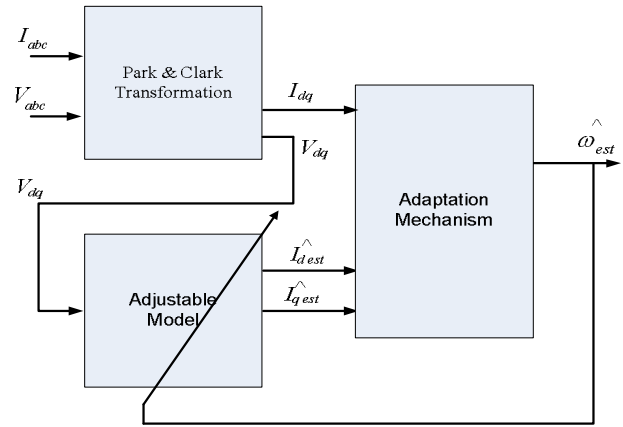


Fig. 2. Configuration of speed and position estimator for a PMSM drives

Firstly, the three-phase voltage and current are converted to d - q model through park and clark transformations. Then, the d - q currents and voltages are being used in Adjustable Model and Adaptation Mechanism respectively. From equation (5) and (6), the Adjustable Model equations can be formulated as below:

$$\frac{d}{dt} i_d = (v_d - r_s i_d + \omega_e L_q i_q) / L_d \quad (11)$$

$$\frac{d}{dt} i_q = (v_q - r_s i_q - \omega_e L_d i_d - \omega_e \Psi_m) / L_q \quad (12)$$

The output of conversion three-phase model is estimated d - q current which is compared with actual d - q axis currents. These currents are used to calculate the estimated speed through adaptation mechanism. The adaptation mechanism is designed in order to improve the stability and behavior of the adaptive system. It is calculated using Popov's hyper-stability theory to derive the estimated speed as in equation (13)

$$\hat{\omega}_{est} = \left(k_p + \frac{k_i}{s} \right) \mathcal{E} \quad (13)$$

$$\mathcal{E} = (i_d \times \hat{i}_{q\ est}) - (i_q \times \hat{i}_{d\ est}) - \frac{\Psi_m}{L} (i_q - \hat{i}_{q\ est}) \quad (14)$$

An estimation error defined by equation (14) is derived when the speed used in the current model is not identical to the actual one without any influence of parameter variation. A tuning signal for the adjustable model is generated from the regulation of this error through a PI controller.

IV. HARDWARE IMPLEMENTATION

The hardware implementation consists of PC, DSP, VSI, optocoupler, PMSM and Hall-effect current sensors. The control board for drive system is dSPACE DSP DS1103. The DSP has been supplemented by a set of on-board peripherals used in digital control systems such as A/D and D/A converters. The DS1103 is equipped with a TMS320F240 that acts as slave processor for advanced I/O purposes. The power circuit of the drives is composed of IGBT based three-phase VSI and gate driver circuits. The specification of VSI is given in Appendix. The VSI is advised to operate at 10kHz maximum switching frequency and can supply up to 46A. The optocoupler (HCPL-3120) are used as protection device to interface the switching signals from DSP controller board to the IGBT modules. The DC link voltage of 300V for the VSI is achieved through three phase diode bridge rectifier module. In this VSI, the dead-time of $3.0\mu\text{s}$ is applied to each switching transition to prevent a shoot-through fault or short-circuit fault. The model of PMSM is BSM90C-2150 from BALDOR. The motor's parameters are presented in Table 1. The Experimental set-up for the overall system is depicted in Fig. 3.



Fig. 3. Experimental set-up for sensorless speed control for PMSM drives

The model, simulation and analysis of the sensorless speed PMSM drives is done using MATLAB/Simulink environment. The model is downloaded to the input/output connection via Real Time (RTI) library. The implementation of the model is carried out on RTI hardware through dSPACE expansion box. After verification in a real environment, the outputs are monitored and tuned through Graphical User Interface (GUI) indSPACE Control Desk. Then the output of the system such as speed, rotor position and three-phase currents are measured and used as system feedback through dSPACE's Analog to Digital (ADC) ports.

V. RESULTS AND DISCUSSION

The variable speed drives responses for sensorless control are investigated through Fig. 4 to Fig. 8. The vector controlled PMSM drives was tested under various operating conditions.

A. Operation from stand-still

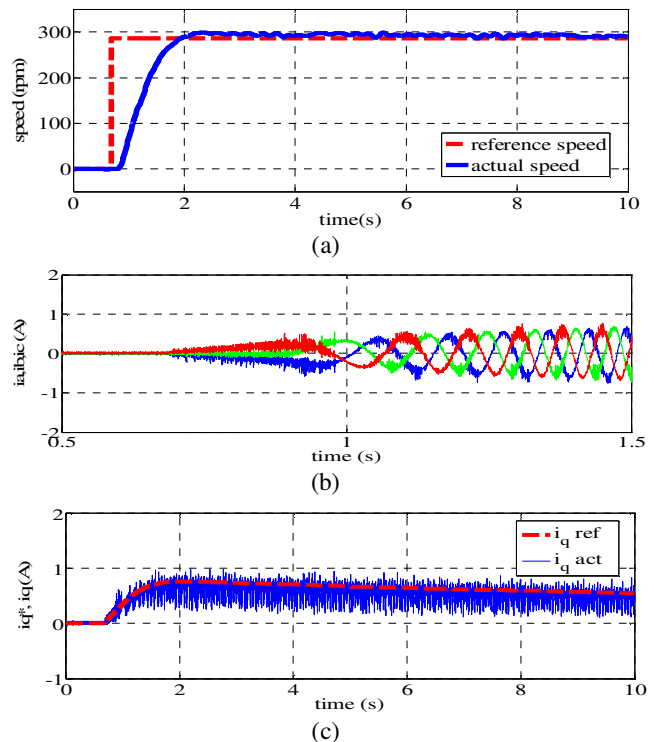
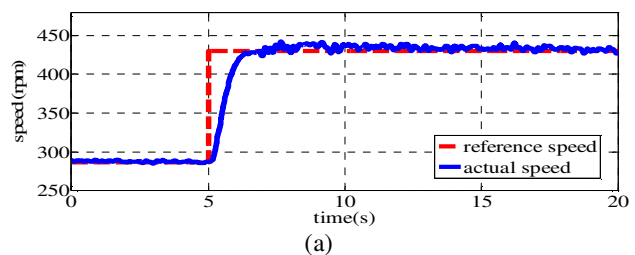


Fig. 4. Experimental results for operation from stand-still; (a) speed response, (b) zoom view of i_a , i_b , and i_c currents at $0.5\text{s} < t < 1.5\text{s}$, (c) quadrature current responses i_q^* and i_{qact}

Fig. 4s show the performance of the PMSM from standstill to 286rpm. This figure proves that the proposed system is able to operate from stand-still and provides good performance in the low speed operation.

B. Increase step command



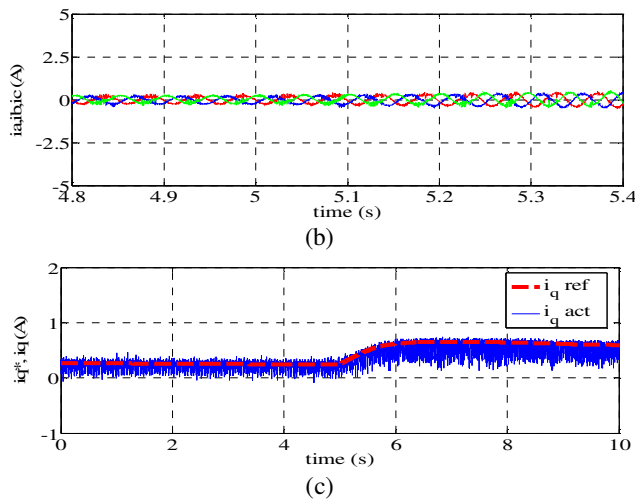


Fig. 5. Experimental results for increase the step command operation; (a) speed response, (b) zoom view of i_a , i_b , and i_c currents at $4.8s < t < 5.4s$, (c) quadrature current responses i_q^* and $i_{q,act}$

Fig. 5 present the experimental result for increasing the step command from 286rpm to 430rpm. The actual speed response follow well the reference input and the three-phase current also shows the slightly changes in magnitude as depicted in Fig. 5(b).

C. Forward to reverse operation

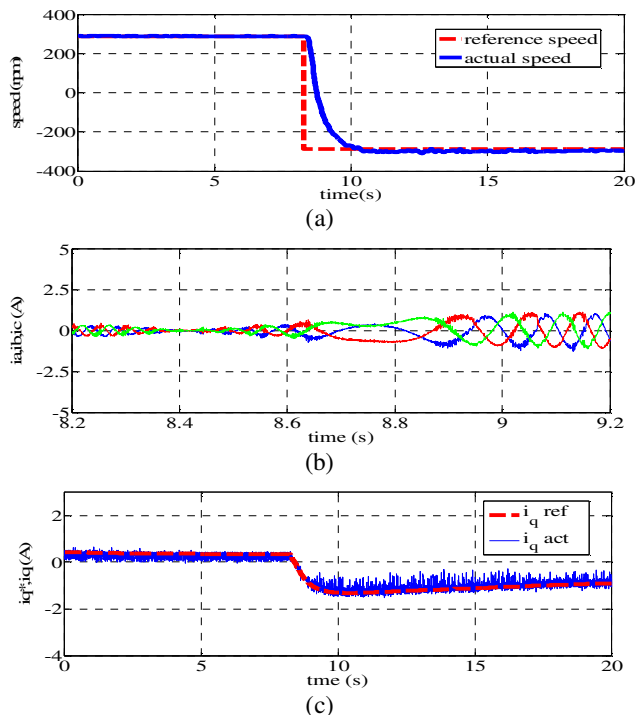


Fig. 6. Experimental results for forward to reverse operation ; (a) speed response, (b) zoom view of i_a , i_b , and i_c currents at $8.2s < t < 9.2s$, (c) quadrature current responses i_q^* and $i_{q,act}$

Fig. 6 presents the robustness of the proposed controller from forward to reverse operations. The PMSM is tested running at 286rpm (forward) to -286rpm (reverse). The system gives good speed response without huge overshoot during the transition.

D. Reverse to Forward Operation

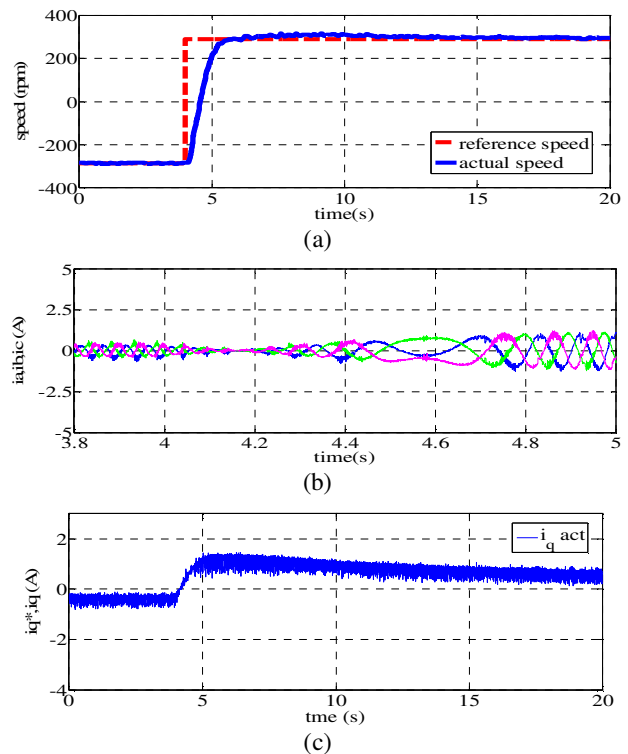
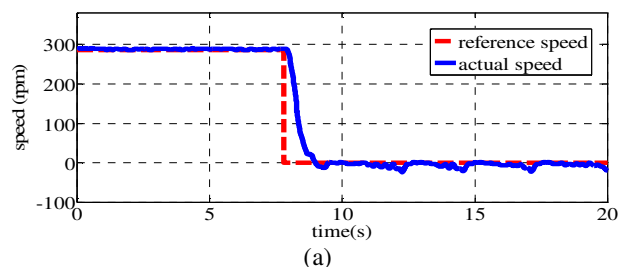


Fig. 7. Experimental results for reverse to forward operation; (a) speed response, (b) zoom view of i_a , i_b , and i_c currents at $3.8s < t < 5s$, (c) quadrature current response i_q^*

The PMSM also tested from reverse to forward operation. The speed response for this test is demonstrated in Fig. 7. Similar with previous test, the speed response do not show any overshoot characteristic and follow the speed reference with acceptable rise time.

E. Zero Speed Command



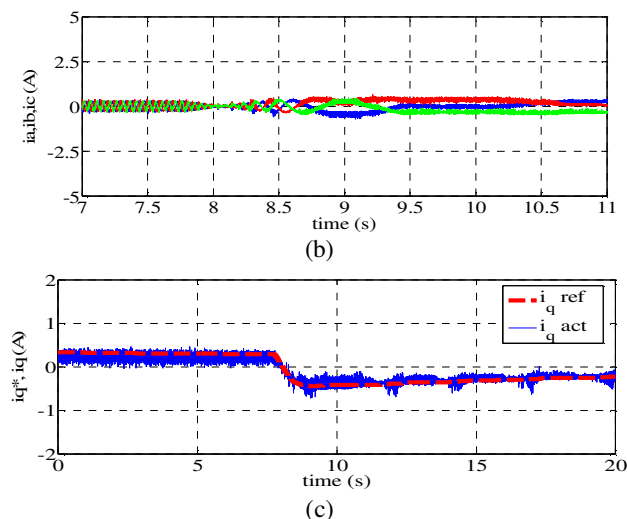


Fig. 8. Experimental results for zero speed operation; (a) speed response, (b) zoom view of i_a , i_b , and i_c currents at $7s < t < 11s$, (c) quadrature current responses i_{q*} and $i_{q,act}$

One of the major issues in sensorless speed drives is the capability of the system during low speed and zero speed operations. Fig. 8 shows that the proposed sensorless speed drives is able to operate during zero speed operation. The speed response may have acceptable ripple due to inaccuracy of the estimator because of the voltage and current values are very small during zero speed operation.

VI. CONCLUSION

The experimental results of the sensorless speed control of PMSM are presented. The test results show the efficiency of the proposed controller for variation of speed and prove that the zero speed operation can be achieved. By using sensorless speed control, the cost and size of the drive system can be reduced thus make this current study significance to the research of the PMSM drives. The effectiveness of the dSPACE DS1103 board is also obtained. The dSPACE board offer "user friendly" features which any correction can be corrected and tuned without any changes in programming..

APPENDIX

TABLE 1 SPECIFICATIONS OF PMSM

No	Motor Specifications	Value
1	Rated Torque	5.2Nm
2	Rated Speed	2000rpm
3	Inertia	0.000881 kgm ²
4	Resistance	5 Ω
5	Inductance	0.0148mH
6	Magnet Flux	0.16374Vs
7	DC Link Voltage	300 V

(i) Specification of VSI.

SEMISTOP Stack, Types: SKS 46F B6U+E1CIF+B6CI 17 V06, Semikron IGBT: SK70 GAL 063, Semikron IGBT driver: SKHI 20opA, Voltage: 300V_{dc}, 350V_{dc}, I_{rms}: 46A, Maximum switching frequency: 10kHz

(ii) Specification of current sensor.

Hall-type Honeywell HY 15-P, Turn ratio: 1/1000, Measured current: 100mA for 100A, Supply voltage: $\pm 15A$

REFERENCES

- [1] K. Iizuka, H. Uzuhashi, M. Kano, T. Endo, and K. Mohri, "Microcomputer control for sensorless brushless motor," *Industry Applications, IEEE Transactions on*, pp. 595-601, 1985.
- [2] F. Genduso, R. Miceli, C. Rando, and G. R. Galluzzo, "Back EMF sensorless-control algorithm for high-dynamic performance PMSM," *Industrial Electronics, IEEE Transactions on*, vol. 57, pp. 2092-2100, 2010.
- [3] S. Ogasawara and H. Akagi, "An approach to position sensorless drive for brushless DC motors," *Industry Applications, IEEE Transactions on*, vol. 27, pp. 928-933, 1991.
- [4] F. M. L. De Belie, P. Sergeant, and J. A. Melkebeek, "A sensorless drive by applying test pulses without affecting the average-current samples," *Power Electronics, IEEE Transactions on*, vol. 25, pp. 875-888, 2010.
- [5] R. Wu and G. R. Slemon, "A permanent magnet motor drive without a shaft sensor," *Industry Applications, IEEE Transactions on*, vol. 27, pp. 1005-1011, 1991.
- [6] M. Eskola and H. Tuusa, "Comparison of MRAS and novel simple method for position estimation in PMSM drives," in *Power Electronics Specialist Conference, 2003. PESC '03. 2003 IEEE 34th Annual*, 2003, pp. 550-555 vol.2.
- [7] M. E. Elbuluk, T. Liu, and I. Husain, "Neural-network-based model reference adaptive systems for high-performance motor drives and motion controls," *Industry Applications, IEEE Transactions on*, vol. 38, pp. 879-886, 2002.
- [8] S. Maiti, C. Chakraborty, Y. Hori, and M. C. Ta, "Model Reference Adaptive Controller-Based Rotor Resistance and Speed Estimation Techniques for Vector Controlled Induction Motor Drive Utilizing Reactive Power," *Industrial Electronics, IEEE Transactions on*, vol. 55, pp. 594-601, 2008.
- [9] A. Rajasekhar, R. K. Jatho, A. Abraham, and V. Snael, "A novel hybrid ABF-PSO algorithm based tuning of optimal FOPI speed controller for PMSM drive," in *The 12th International Conference on Carpathian Control (ICCC2011)*, Velke Karlovice 2011, pp. 320-325.
- [10] P. Vas, *Artificial-intelligence-based electrical machines and drives: application of fuzzy, neural, fuzzy-neural, and genetic-algorithm-based techniques*: Oxford University Press, USA, 1999.
- [11] P. Vas, *Vector control of AC machines*: Clarendon press Oxford, 1990.
- [12] B. K. Bose, *Modern power electronics and AC drives*: Prentice Hall PTR USA, 2002.
- [13] P. Vas, *Sensorless vector and direct torque control* vol. 9: Oxford university press Oxford, UK, 1998.
- [14] W. Leonhard, *Control of electrical drives*: Springer Verlag, 2001.
- [15] P. Pillay and R. Krishnan, "Modeling, simulation, and analysis of permanent-magnet motor drives. I. The permanent-magnet synchronous motor drive," *IEEE Transactions on Industry Applications*, vol. 25, pp. 265-273, 1989.
- [16] P. Pillay and R. Krishnan, "Modeling, simulation, and analysis of permanent-magnet motor drives. I. The permanent-magnet synchronous motor drive," *Industry Applications, IEEE Transactions on*, vol. 25, pp. 265-273, 1989.